

# Effect of extracellular vesicles derived from ADPKD-patient urine on the proliferation of human cystic renal epithelial cells

Cameron Lozano

16 May 2025

## Abstract

Autosomal dominant polycystic kidney disease (ADPKD), the most common genetic cause of kidney failure, involves the formation and expansion of fluid-filled cysts in the kidney and other organs throughout a patient's lifetime. The disease results from a pathogenic variant in either allele of one of two genes, *PKD1* or *PKD2*, which causes a host of changes in renal tubular epithelial cells, including increased proliferation and defects in planar cell polarity. How the pathogenic variants induce these changes, however, is not well understood. Recent evidence has suggested that extracellular vesicles (EVs) released from cystic renal tubular epithelial cells may play a central role by promoting cystic behavior in neighboring tubular epithelial cells. We investigated whether this could be observed in an *in vitro* model of human ADPKD, hypothesizing that cystic renal epithelial cells would exhibit more proliferation after treatment with EVs derived from the urine of ADPKD patients than after treatment with EVs derived from the urine of healthy controls. Although the cystic epithelial cells in our experiment were unintentionally cultured under cytotoxic conditions and so we could not observe changes in normal proliferation, we were still able to investigate whether the EV treatments promoted cystic behavior by using cell survival as an alternative outcome to proliferation. Within this setting, we found that (a) treatment with urinary EVs significantly increased the survival of cystic cells relative to the survival of untreated cystic cells over 48 hours, (b) cells treated with urinary EVs derived from ADPKD patients exhibited significantly greater increases in survival than cells treated with urinary EVs derived from a healthy individual, and (c) the strength of this effect of patient-derived urinary EV treatments on cell survival was dependent on both the dose of EVs used and the gene responsible for ADPKD (*PKD1* or *PKD2*) in the patient from whom the EVs were derived. Overall, our findings support the proposed role of EVs in the pathophysiology of ADPKD and suggest several ways in which this role can be more thoroughly investigated in future work.

## Contents

1 Introduction	2
2 Results	8
3 Discussion	14
4 Materials and methods	19
5 Acknowledgments	25
References	26

## 1 Introduction

### 1.1 Epidemiology, clinical manifestations, and treatments in ADPKD

Autosomal dominant polycystic kidney disease (ADPKD) is the most common inherited kidney disorder in the world, with an incidence of 1 in 500 to 1 in 1000 people.<sup>1</sup> The disorder is also the fourth leading cause of end-stage kidney disease (ESKD) in the world, with approximately seven in ten patients progressing to ESKD in their lifetimes, at a median age of 58.<sup>1</sup> ADPKD occurs in all ethnicities, and, although it affects both sexes at equal rates, the risk of progression to ESKD is about 21% greater for men.<sup>2</sup>

ADPKD patients typically present with clinical manifestations in their third or fourth decade of life,<sup>3</sup> though some have been observed to present with enlarged kidneys, cysts, and other manifestations *in utero*.<sup>4</sup> The primary effect of the genetic defects that cause ADPKD is the formation of fluid-filled cysts in the kidneys and other organs, including the liver (with 80% of patients demonstrating polycystic liver disease by the age of 30), pancreas (in 10%), and seminal vesicles (in up to 40% of male patients).<sup>2</sup> In the kidney, cysts originate from renal tubular epithelial cells at all locations of the nephron as well as the glomerulus and are lined by a monolayer of cells that are more proliferative and less differentiated than healthy tubular epithelial cells.<sup>3</sup> Cysts form and grow in size continuously throughout a patient's lifetime, resulting in a plethora of clinical manifestations caused primarily by kidney enlargement and eventual decline in kidney function. These clinical manifestations can vary substantially in incidence and severity but generally include defects in urinary concentration, acute and chronic flank pain (one of the most common and earliest-manifesting symptoms), hypertension (with a median age of onset of 27 years), urinary tract infections, hematuria, kidney stones, and intracranial aneurysms (in 9% of patients overall and in 22% of patients with a family history of ruptured intracranial aneurysms).<sup>1,2,5</sup> Although the disorder is typically not diagnosed until late in the second decade to the third decade of life,<sup>6</sup> about 2% of ADPKD patients begin to manifest clinical

symptoms before the age of 15.<sup>7</sup>

Kidney disease is highly variable, but, for most ADPKD patients, the decline in kidney function does not begin until the fourth decade of life, at which point the kidneys are substantially enlarged, with little recognizable, functional renal tissue still visible via imaging.<sup>8</sup> Progression to ESKD typically occurs 5 to 10 years after this functional decline begins,<sup>3</sup> after which patients must undergo renal replacement therapy in the form of transplantation, hemodialysis, or peritoneal dialysis for continued survival.<sup>9</sup>

## 1.2 Genetics and pathophysiology

Perhaps the most remarkable aspect of ADPKD is its namesake Mendelian genetics: in the overwhelming majority of patients, the disorder results from a single pathogenic variant in a single allele of one of two genes, *PKD1* (responsible for 78% of cases) or *PKD2* (15%),<sup>10</sup> which encode the proteins polycystin-1 (PC1) and polycystin-2 (PC2), respectively. Patients with a *PKD2* disease-causing variant demonstrate similar clinical manifestations as *PKD1* patients, but *PKD2* patients tend to experience milder kidney disease, with fewer renal cysts, delayed onset of hypertension, delayed ESKD by approximately twenty years, and longer overall survival.<sup>9,11</sup> Disease severity in *PKD1* patients has also been shown to correlate strongly with the type of pathogenic variant: patients with truncating mutations (i.e., large rearrangements and frameshift, nonsense, and splice mutations) are 2.74 times more likely to experience ESKD in their lifetimes than patients with non-truncating mutations (i.e., in-frame and missense mutations), progressing to ESKD at a median age twelve years younger.<sup>11</sup> In addition, whereas disease severity in patients with truncating mutations is significantly correlated with sex, with males progressing to ESKD at a median age 4.9 years younger than females, no such correlation between age at ESKD and sex has been observed for patients with non-truncating mutations.<sup>11</sup> ADPKD research must therefore pay special attention to these variations in genetic factors; for brevity, this paper will use a condensed nomenclature for differentiating patients by their pathogenic variants, described in Table 1.

Site of pathogenic variant	Variant type	Designation
<i>PKD1</i>	Truncating	ADPKD- <i>PKD1</i> <sub>tr</sub> patient
	Non-truncating	ADPKD- <i>PKD1</i> <sub>nt</sub> patient
<i>PKD2</i>	Truncating	ADPKD- <i>PKD2</i> <sub>tr</sub> patient
	Non-truncating	ADPKD- <i>PKD2</i> <sub>nt</sub> patient

Table 1: Nomenclature used in this paper to differentiate ADPKD patients by the location and type of pathogenic variant they carry. Adapted from the 2025 Kidney Disease: Improving Global Outcomes (KDIGO) guidelines,<sup>12</sup> with the addition of a subscript identifying variant type. When variant type is not relevant to the proceeding discussions, the subscript will be omitted.

Both polycystins are cell-membrane proteins. PC1, a large protein of about 463 kDa with eleven trans-

membrane domains, likely functions as an adhesion molecule and receptor for a recently-identified ligand variously referred to as exosomal polycystin-1 interacting protein (EPCIP) or as CU062,<sup>1,8,13,14</sup> while PC2, about 110 kDa with six transmembrane domains, functions as a non-selective, calcium-permeable cation channel.<sup>1,8</sup> Together, they form a functional polycystin-complex which localizes to the primary cilia of renal tubular epithelial cells, where it has been suggested that the complex acts as a mechanosensor which performs a number of functions, including regulating the influx of Ca<sup>2+</sup> on the apical surface of epithelial cells in response to changes in urine flow.<sup>8,15</sup> Influx of Ca<sup>2+</sup> to renal epithelial cells inhibits the activity of adenylyl cyclase 6 (AC6), which results in a decrease in intracellular cyclic adenosine monophosphate (cAMP) levels.<sup>2</sup> Dysfunctions in the polycystin-complex therefore reduce Ca<sup>2+</sup> influx, which results in increased activity of AC6 and accumulation of intracellular cAMP, which in turn stimulates mitogen-activated protein kinase and extracellularly regulated kinase (MAPK/ERK) signaling and leads to cyst expansion by increasing epithelial cell proliferation, fluid secretion, and interstitial inflammation.<sup>1,8</sup> This primary cilium-based role of PC1 and PC2 in regulating intracellular Ca<sup>2+</sup> and cAMP levels is hypothesized to be a key mechanism by which *PKD1* and *PKD2* loss-of-function mutations result in the generation and enlargement of renal cysts in ADPKD.<sup>15</sup> Both proteins' functions likely extend beyond the primary cilia as well; PC1 additionally localizes to focal adhesions, desmosomes, and adherens junctions in the basolateral epithelial membrane (likely having a role in the regulation of cell-to-cell contact and the inhibition of proliferation) and PC2 additionally localizes to the endoplasmic reticulum.<sup>8</sup> The numerous observed functions of PC1, PC2, and the polycystin-complex have given rise to many competing hypotheses describing the pathophysiology connecting mutations in *PKD1* and *PKD2* to the formation and expansion of cysts in ADPKD beyond disruptions in the cAMP pathway. These hypotheses suggest that cyst formation occurs due to disruptions in the mammalian target of rapamycin (mTOR) pathway, in the Janus kinase-signal transducers and activators of transcription (JAK-STAT) pathway, and in the Wnt signaling pathways, among others.<sup>16</sup> How all of these proposed disruptions contribute to the mechanisms by which *PKD1* and *PKD2* loss-of-function mutations result in cyst formation and expansion remains incompletely understood.

The reason for which inheritance of a single mutated allele of *PKD1* or *PKD2*, rather than inheritance of two mutated alleles, is sufficient to produce cyst formation and expansion also remains unclear. Two primary hypotheses seek to explain this phenomenon. The “two-hit” hypothesis follows from the observation that, despite the inherited, germ-line mutation existing in all renal epithelial cells of an ADPKD patient, fewer than 1% of these cells develop into cysts; it suggests that a single *PKD1* or *PKD2* mutation is insufficient for cyst formation, which instead only takes place when a second, somatic mutation occurs in the functional allele of a renal epithelial cell.<sup>17</sup> More recent research, however, has suggested that a “haploinsufficiency” hypothesis is more likely.<sup>8</sup> This hypothesis, which draws on observations that reduced levels of PC1 or

PC2 (rather than full knock-outs of the proteins) are sufficient to produce the clinical manifestations of ADPKD, suggests that cysts form when the single germ-line mutation in *PKD1* or *PKD2* reduces the levels of functional PC1 or PC2 below a certain threshold, which can vary per-cell depending on other pathways, extracellular conditions, signaling from nearby epithelial cells, and other factors.<sup>8,18</sup>

### 1.3 Extracellular vesicles and ADPKD

Extracellular vesicles (EVs) are small (30-150 nm), membrane-contained vesicles released by prokaryotic and eukaryotic cells.<sup>19,20</sup> EVs are produced and exported from a cell by one of three distinct mechanisms: via direct outward budding and fission of the plasma membrane (these EVs typically being called microvesicles or ectosomes), via the fusion of endosomal-network-derived multi-vesicular bodies (MVBs) with the plasma membrane (these EVs typically being called exosomes), or via blebbing of the plasma membrane of cells undergoing apoptosis (these EVs typically being called apoptotic bodies).<sup>19</sup> Their release and interaction with other cells, both near and remote to the EVs' cells of origin, has been identified as a crucial component of information-transfer between cells. This information – the cargo of EVs – can take the form of proteins, lipids, DNA, RNA, and sugars, making these vesicles one of the most versatile discovered methods of cell-to-cell communication.<sup>19</sup> EVs have been implicated in a host of biological processes, from alteration of protein expression levels, to regulation of immune responses, to enhancement of plasma coagulation, to elimination of cellular waste materials, and many more.<sup>19</sup>

Intense and recent investigation has also implicated EVs in the progression of numerous human diseases. In cancer, for example, tumors have been found to actively produce and release EVs; upon contact with non-cancerous target cells, the EVs reprogram these cells to contribute to angiogenesis, thrombosis, metastasis, and immunosuppression.<sup>21</sup> EVs have also been hypothesized to facilitate the spread of misfolded proteins between neurons in the progression of Parkinson's disease.<sup>22</sup>

Within the last few years, research has implicated EVs in the progression of ADPKD, as well. EVs isolated from human urine, which originate from renal epithelial cells in the glomerulus, proximal tubule, thick ascending limb of Henle, distal convoluted tubule, and collecting duct,<sup>19</sup> have been found to contain the polycystin-complex formed from PC1 and PC2 in their membranes.<sup>13,23</sup> Urinary EVs from ADPKD-*PKD1* patients have been found to contain nearly half the levels of PC1 and PC2 (54% and 53%, respectively) compared to urinary EVs from unaffected healthy individuals, mirroring the loss of function of one of the two *PKD1* alleles and, in turn, the expected reduction in the functional levels of the polycystin-complex.<sup>23</sup> While the initial primary implication of this discovery was that the levels of PC1 and PC2 in urinary EVs could be used as biomarkers for diagnosing and monitoring the progression of ADPKD,<sup>23</sup> later work by Ding

et al. (2021)<sup>20</sup> suggested further implications. The authors showed that EVs derived both from cystic renal epithelial cell cultures and from human ADPKD patient urine not only carried different cargo compared to EVs derived from non-cystic cultures and healthy individuals' urine (respectively) but also directly promoted the growth of cysts in mouse kidneys and in healthy renal tubular epithelial cell cultures. This suggested that EVs derived from the epithelia of nephrons in ADPKD patients can serve not only as biomarkers of the disease but also as key promoters in the development of kidney cysts and the progression of the disease itself.<sup>20</sup>

In December 2024, building on this and other growing evidence for a functional role of EVs in ADPKD pathophysiology, Hogan and Ward<sup>13</sup> published a compelling hypothesis which places EVs in a central role in the genesis of renal cysts in ADPKD. Their proposition draws on a host of evidence from prior research, including (a) that dysfunctions in the primary cilia of renal tubular epithelial cells are critical for the formation of cysts in ADPKD; (b) that the localization of PC1 and PC2 to the primary cilium appears “vesicular in nature” via deconvolution confocal microscopy, with hollow EVs embedded with polycystin-complexes and applied to the shaft of the primary cilium; and (c) that mutations in PC1 or PC2 are also associated with a variety of non-cystic phenotypes that cannot reasonably be explained by changes in primary cilium signaling, such as resistance to carcinoma development and defects in cystic cells’ mitochondrial function.<sup>13</sup> Attempting to explain these seemingly contradicting observations, Hogan and Ward propose an “EV theory”-based hypothesis for the pathophysiology of ADPKD, which predicated itself on two ideas: first, that the polycystin-complex is involved in the biogenesis of EVs that themselves have polycystin-complexes embedded in their vesicular membranes, and, second, that the critical role of the primary cilium in ADPKD is that of a *receptor* for these polycystin-complex-containing EVs.<sup>13</sup> They thus hypothesize that the polycystin-complex generates new polycystin-containing EVs – potentially for the primary purpose of transporting lipid-modified (and thus poorly water-soluble) Wnt proteins, the non-canonical signaling pathway of which is critical for establishing planar cell polarity – and that the primary cilia of other renal epithelial cells then bind to these EVs and allow their contents into the cell (by some unknown mechanism) where they can transduce various signals. This hypothesis provides a novel explanation for why dysfunctions either in the polycystin-complex or in the primary cilium are critical for cyst formation and expansion; the dysfunctions would inhibit EV-dependent signal transduction pathways and thereby alter levels of key intracellular proteins, resulting in cyst formation via disruption of planar cell polarity (due to altered levels of Wnt proteins) and in cyst expansion via increased cell proliferation (due to altered levels of phosphorylated protein kinase B and ERK, for example, both of which have been shown to be elevated in renal epithelial cells treated with *PKD1*-null EVs<sup>20</sup>). It would also explain why mutations in the polycystin-complex proteins can produce physiological changes unrelated to the primary cilium: the mutations would inhibit the biogenesis

of EVs in specific contexts that may require the use of EVs for normal function (for example, the resistance to carcinoma development in ADPKD may be due to an inhibition of the observed process of cancer cells generating EVs containing mRNAs that, when taken in by normal fibroblasts, reprogram the fibroblasts to become supportive tumor-associated fibroblasts).<sup>13</sup>

Although this “EV theory” of ADPKD pathophysiology hypothesizes additional roles for EVs beyond the increase in epithelial cell proliferation that in part leads to the formation and growth of cysts, this foundational effect of EVs has not yet been concretely established in a murine or human ADPKD model. The aforementioned 2021 study by Ding et al.<sup>20</sup> has made the greatest progress so far. Firstly, the authors demonstrated that the treatment of normal mouse renal collecting duct epithelial cell cultures (mIMCD3 cells) with EVs derived from *PKD1*-null renal proximal tubule epithelial cells (PN24 cells) produces significantly greater expression of cell proliferation marker PCNA (proliferating cell nuclear antigen) in the treated cells compared to in untreated cells. Secondly, the authors demonstrated that the treatment of normal mIMCD3 cell cultures with EVs derived from the urine of human ADPKD patients similarly produces significantly greater cell proliferation compared to treatment with EVs derived from the urine of healthy individuals.<sup>20</sup>

Despite these advancements by Ding et al.,<sup>20</sup> several aspects of the impact of EVs on renal epithelial cell proliferation in the context of ADPKD remain unclear. Firstly, because Ding et al.<sup>20</sup> examined the effect of human urinary EVs on mouse cell cultures, it is unknown whether the effect also exists in a more physiologically representative model, wherein the urinary EVs and renal tubular epithelial cell cultures are derived from the same species. Secondly, because Ding et al.<sup>20</sup> studied the effect of cystic-cell-derived EVs on normal (i.e., non-cystic) cell cultures, it is unknown whether the effect also exists in an explicitly ADPKD-based model – in other words, a model wherein EVs with *PKD1* or *PKD2* mutations are taken in by *cystic* cell cultures which also have a *PKD1* or *PKD2* mutation, as would be the case in the hypothesized model of EV-driven progression of ADPKD in patient kidneys.

## 1.4 Aims and experimental approach

In this project, we investigated whether the behavior of a more representative ADPKD model supports Hogan and Ward’s<sup>13</sup> “EV theory”. Specifically, our model involved the treatment of human cystic renal epithelial cells – which had a truncating *PKD1* mutation – with EVs derived either from the urine of ADPKD patients (one ADPKD-*PKD1*<sub>tr</sub> patient and one ADPKD-*PKD2*<sub>tr</sub> patient) or from the urine of an unaffected healthy individual. Within this setting, we sought to determine (a) whether co-incubation with human urinary EVs derived from ADPKD patients increases the proliferation of human cystic renal epithelial cells more than

co-incubation with urinary EVs derived from unaffected healthy individuals, as well as whether the extent of this increase in proliferation is dependent on (b) the dose of EVs used and/or (c) the location (*PKD1* or *PKD2*) of the germ-line mutation carried by the ADPKD patient from whom the urinary EVs are derived.

Hogan and Ward's<sup>13</sup> EV theory suggests that our findings should agree with those of Ding et al.<sup>20</sup> Expecting this to be the case, we hypothesized that when cystic renal epithelial cells are co-incubated with urinary EVs, the cells treated with ADPKD patient-derived EVs would exhibit more proliferation than those treated with healthy individual-derived EVs, and this effect would be even more pronounced in cells treated with EVs at higher doses. Because ADPKD-*PKD1* patients tend to experience more severe kidney disease than ADPKD-*PKD2* patients,<sup>9,11</sup> we also hypothesized that urinary EVs derived from an ADPKD-*PKD1* patient would produce a greater increase in cell proliferation than urinary EVs derived from an ADPKD-*PKD2* patient.

While our experimental design focused solely on increased proliferation as a measure of cystic behavior, it should be noted that “cystic behavior” is a broad outcome which also encompasses dysfunctions in the establishment of planar cell polarity, reduced cell death from nutritional stress, and altered metabolic pathways, among other changes. Increased proliferation is only one piece of the broader mosaic of mechanisms by which EVs may promote the formation and expansion of kidney cysts. This limitation in perspective, however, fortunately provided us the flexibility to investigate a different cystic behavior outcome – cell *survival* – when our culture conditions unintentionally did not facilitate normal cell proliferation.

## 2 Results

### 2.1 Isolated urinary EVs contain characteristic markers and are normal in size and morphology

We first ensured that our protocol for isolating EVs from human urine (Figure 1a) was successful in collecting undamaged EVs. The presence of CD9 and CD81, two tetraspanins which are reliable marker for EVs,<sup>24,25,26</sup> in EV isolations from several different urine samples (Figure 1b) confirmed that our protocol did capture EVs. While we also attempted to detect the presence of PC1 and PC2 in the EV isolations via western blot, our attempts were unsuccessful, likely due to the large size and relatively delicate structure of the two proteins – we intend to verify the presence of PC1 and PC2 in the EV isolations via mass spectrometry proteomic analyses in the near future. Visual assessment of negative stain electron microscopy images (Figure 1d) – captured by trained technicians at The University of Chicago Advanced Electron Microscopy Core Facility – confirmed that the EVs were undamaged, morphologically normal, and not co-isolated with

problematic polymers of Tamm-Horsfall protein (THP/uromodulin). Nanoparticle-tracking analysis (NTA) of EVs isolated from a patient urine sample (Figure 1c) confirmed that the particles isolated had diameters within the expected range for EVs (generally 30-150 nm), with a mode of  $116.3 \pm 6.5$  nm and with 50% of particles having diameters less than 134 nm.

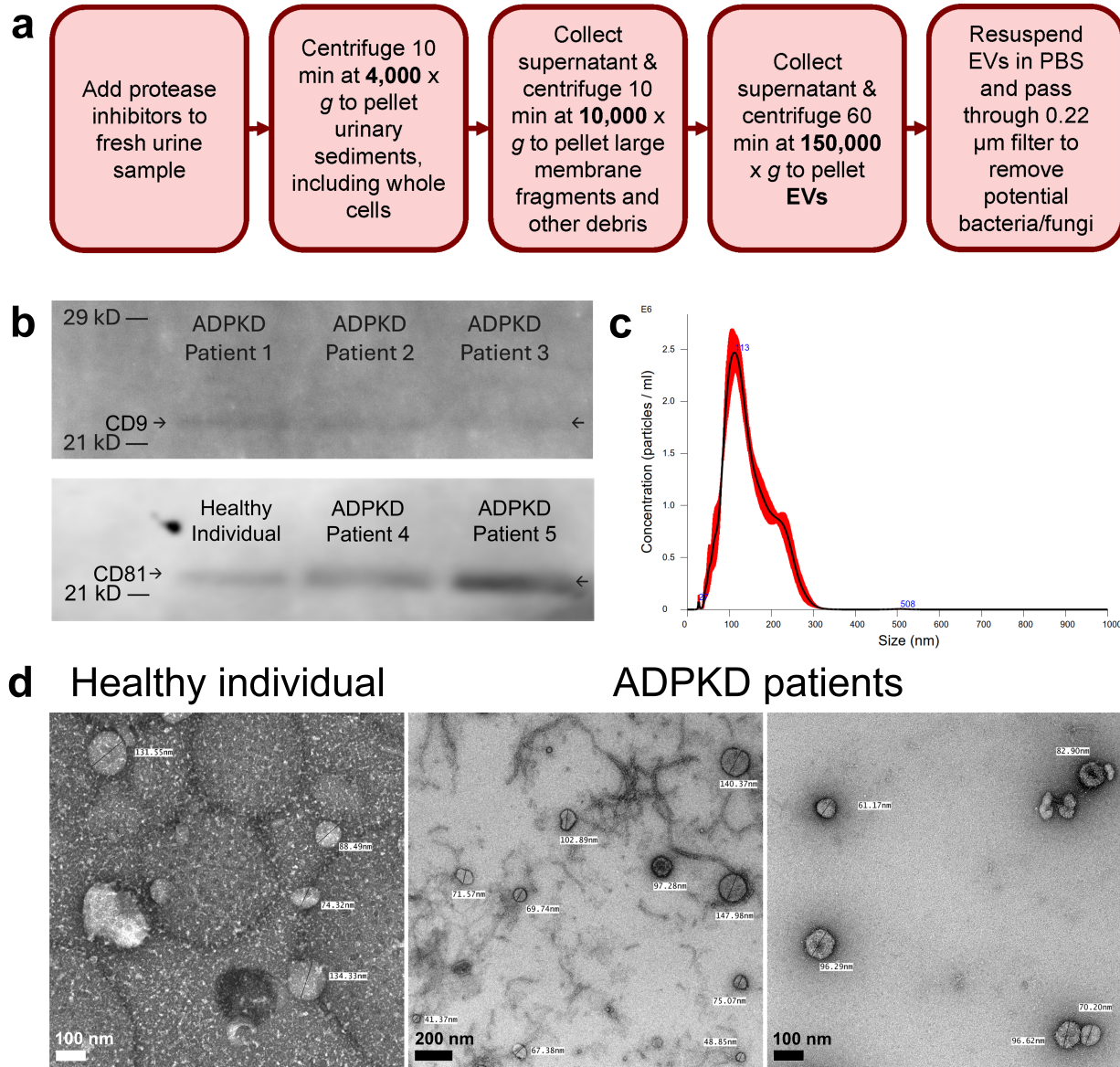


Figure 1: Isolation of renal epithelium-derived extracellular vesicles (EVs) from human urine. **(a)** Isolation protocol. Greater detail in Section 4. **(b)** Western blots of EV isolations from urine samples of one healthy individual and five ADPKD patients for tetraspanin EV markers<sup>24,26</sup> CD9 (top) and CD81 (bottom), indicating the presence of EVs. **(c)** Results of nanoparticle tracking analysis (NTA) for one representative patient-derived urinary EV isolation sample (see Table 2). Red error outline represents  $\pm 1$  standard error of the mean. **(d)** Negative stain electron microscopy (EM) images of EV isolations from one healthy individual's urine sample (left) and from two ADPKD patients' urine samples (middle and right). Differences in background between the images are due to slight variances in the cleaning of the microscope and are unlikely to indicate true substantial differences in isolation sample contents. Variation in observed EV size (labeled) is within normal range.

## 2.2 Relative-survival of renal epithelial cells under starvation and cytotoxic conditions is increased by treatment with ADPKD patient-derived urinary EVs

To investigate the effect of co-incubation with urinary EVs on cystic renal epithelial cell proliferation, we performed a 72-hour cell viability experiment, using an XTT assay (2,3-Bis-(2-Methoxy-4-Nitro-5-Sulfophenyl)-2H-Tetrazolium-5-Carboxanilide assay) to determine changes in cell populations every 24 hours after EVs were added, under starvation conditions (see Section 4 for more details on the cell line, culture media, treatment groups, and protocols).

The starvation condition of 0.1% fetal bovine serum (FBS) was chosen following a similar XTT-based cell viability experiment (Figure 2a) wherein the same cell line was incubated for the same lengths of time in culture media with various concentrations of FBS (and no EVs). We found that a concentration of 0.1% was most effective at starving the cells (i.e., reducing their growth rate) while still allowing for net growth over 72 hours, and as such would allow the most reliable observation of any potential change in proliferation caused by EV treatments.

In the subsequent experiment which implemented the EV treatments, however, the cells behaved differently: cell populations in all treatment groups (including untreated cells) decreased drastically over time, with several groups (including untreated) having average populations of zero after 72 hours (Figure 2b). This is in stark contrast to the prior FBS-focused experiment, in which cells cultured in media with the same FBS concentration experienced an *increase* in population size of about 65.9% on average over 72 hours.

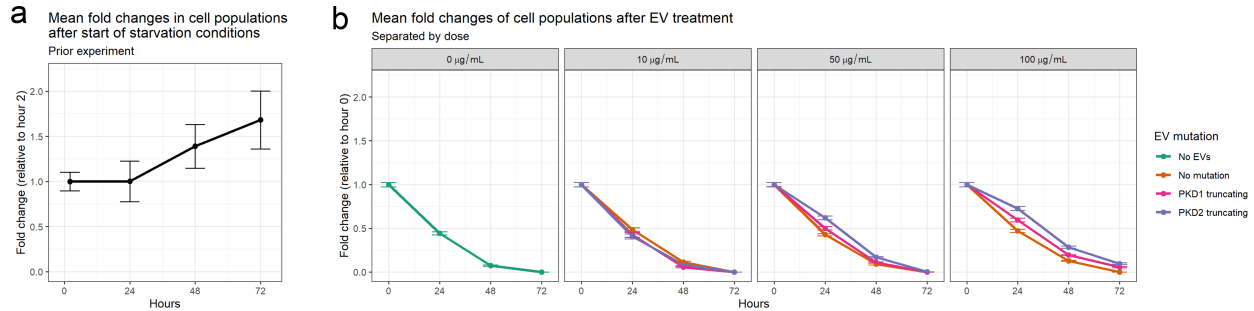


Figure 2: Comparison of cell population changes over time between an earlier preliminary experiment and the primary extracellular vesicle (EV) treatment experiment. **(a)** Mean fold change over 72 hours of untreated immortalized human cystic renal epithelial cells in culture media containing 0.1% fetal bovine serum (FBS) by volume (starvation conditions), relative to cell populations at 2 hours after starvation began.  $n = 36$  for the measurement at 0 hours, and  $n = 6$  per treatment group for measurements at other time-points. An average increase in population size of about 65.9% was observed after 72 hours. **(b)** Mean fold change over 72 hours of the same epithelial cell line in culture media containing the same FBS concentration, but with the addition of treatment with urinary EVs (in the three rightmost boxes; no EVs added in leftmost box), relative to the cell populations at the time EV treatment began (hour 0). Lines are grouped into boxes by the dose of EVs added and colored according to the mutation (or lack thereof) in *PKD1* or *PKD2* possessed by the individual from whom each urine sample was derived.  $n = 60$  for the measurement at 0 hours, and  $n = 6$  per treatment group for measurements at other time-points. Error bars represent  $\pm 1$  standard error.

That even the untreated group of cells experienced this population decline suggests an unintentional difference in conditions between the FBS experiment and the EV experiment as the cause, rather than the EV treatments themselves. Two potential explanations seem most likely. First, while the immortalized human cystic epithelial cells used in the EV experiment belong to the same line as those used in the FBS experiment, the EV experiment's cells were thawed from a different batch, and thus may have been contaminated by some bacteria or fungus that the FBS experiment's cells were not. Although the cell culture used in the EV experiment did exhibit particles suspended in the media upon visual inspection before the experiment was performed, the media did not display typical signs of contamination (such as cloudiness or a color change), and the particles did not appear to exhibit active movement or recognizable bacterial morphology under a microscope, so it was assumed that the particles were simply cell debris. While it is still possible that the culture was compromised by less obvious contaminants, and future experiments should take more care to ensure this is not the case, we do not believe it is the most likely explanation for the cell death observed. Second, a higher concentration of amphotericin B (an antifungal compound) was added to the cell culture media used in the EV experiment than to the media used in the FBS experiment (6.25 µg/mL in EV experiment media compared to 2.50 µg/mL in FBS experiment media), as a heightened precaution against contamination. Amphotericin B is toxic to renal epithelial cells at sufficiently high concentrations, significantly promoting apoptosis at concentrations as low as 1.0 µg/mL,<sup>27</sup> and so this change in media composition may have produced the cytotoxic effect that contributed to the observed cell death.

While the unexpected rates of cell death in our experiment prevent us from reliably assessing EV-induced changes in cell proliferation under normal conditions, they do provide an opportunity to examine the effects of the various treatments on cell survival under cytotoxic conditions. Regardless of the cause of the observed cytotoxicity, because the cells of every treatment group were seeded from the same source and incubated under the same conditions (aside from the differences in EV treatments), we can be confident that significant differences in cell survival between groups were caused by the differences in EV treatments.

Our results (Figure 3) do suggest a positive impact of ADPKD patient-derived urinary EV treatments at doses of 50 µg/mL and 100 µg/mL on the cells' relative-survival, where we define "relative-survival" as the ratio of the surviving population of treated cells to that of untreated cells at the same time-point (see Equation 1 in Section 4.6). Cells treated with urinary EVs derived from an ADPKD-*PKD2*<sub>tr</sub> patient at doses of both 50 and 100 µg/mL experienced significantly greater relative-survival than did cells treated with urinary EVs derived from a healthy individual, at both 24 and 48 hours after treatment ( $p < 0.005$ ). Cells treated with urinary EVs derived from an ADPKD-*PKD1*<sub>tr</sub> patient at a dose of 100 µg/mL also experienced significantly greater relative-survival than did cells treated with urinary EVs derived from a healthy individual, at both 24 and 48 hours after treatment ( $p < 0.005$ ), but those treated at a dose of 50

$\mu\text{g}/\text{mL}$  only experienced significantly greater relative-survival at 24 hours after treatment ( $p < 0.05$ ).

Notably, this “rescuing” effect on cell survival caused by treatment with patient-derived urinary EVs was significantly stronger at a dose of 100  $\mu\text{g}/\text{mL}$  than at a dose of 50  $\mu\text{g}/\text{mL}$  and was significantly stronger at a dose of 50  $\mu\text{g}/\text{mL}$  than at a dose of 10  $\mu\text{g}/\text{mL}$  for urinary EVs derived from both patients and at both 24 and 48 hours ( $p < 0.005$  except for ADPKD-*PKD1<sub>tr</sub>* EVs at 24 hours, where  $p = 0.008$  for 100  $\mu\text{g}/\text{mL}$  vs. 50  $\mu\text{g}/\text{mL}$  and  $p = 0.033$  for 50  $\mu\text{g}/\text{mL}$  vs. 10  $\mu\text{g}/\text{mL}$ ), heavily suggesting the effect is dose-dependent. Evidence for a similar dose-dependency of the rescuing effect of healthy individual-derived EVs is less convincing: the effect was significantly stronger at a dose of 100  $\mu\text{g}/\text{mL}$  than at a dose of 50  $\mu\text{g}/\text{mL}$  ( $p < 0.05$ ), but it was not significantly stronger at a dose of 100  $\mu\text{g}/\text{mL}$  than at a dose of 10  $\mu\text{g}/\text{mL}$ , nor stronger at a dose of 50  $\mu\text{g}/\text{mL}$  than at a dose of 10  $\mu\text{g}/\text{mL}$ .

In addition, the effect of urinary EVs derived from the ADPKD-*PKD2<sub>tr</sub>* patient was significantly stronger than the effect of urinary EVs derived from the ADPKD-*PKD1<sub>tr</sub>* patient, at both 24 and 48 hours and for both 50 and 100  $\mu\text{g}/\text{mL}$  doses ( $p < 0.005$  except for the 50  $\mu\text{g}/\text{mL}$  dose at 24 hours, where  $p = 0.0051$ ), suggesting that the strength of the effect is also impacted by the gene at which the mutation occurs.

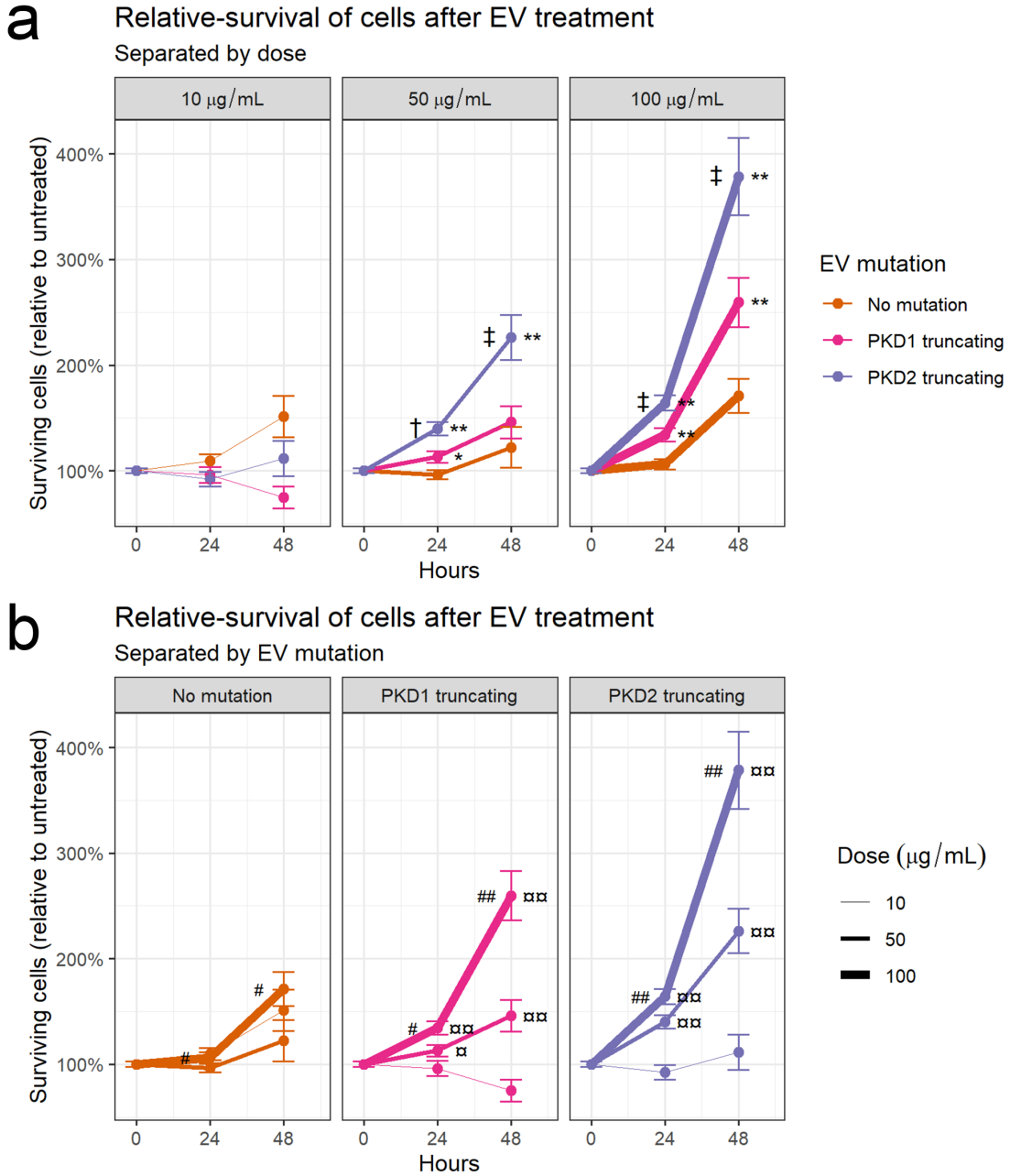


Figure 3: Mean relative-survival of immortalized human cystic renal epithelial cells cultured under cytotoxic conditions over 48 hours after treatment with human urinary extracellular vesicles (EVs). The same data is presented in both (a) and (b), but with different visual arrangements. Line color corresponds to the mutation in *PKD1* or *PKD2* (if any) carried by the individual from whom the urinary EVs were derived (see Table 2 for specific variants), and line thickness corresponds to the dose of EVs used to treat the cells, in  $\mu\text{g}$  of total isolated protein per mL of final well volume.  $n = 60$  for the measurement at 0 hours, and  $n = 6$  per treatment group for measurements at other time-points. While populations of all groups were also measured at 72 hours after treatment, no living cells remained in the untreated group, making relative-survival calculations at this time-point impossible. Error bars represent  $\pm 1$  standard error.

\*  $p < 0.05$  and \*\*  $p < 0.005$  vs. same dose of EVs derived from a healthy individual.

†  $p < 0.05$  and ‡  $p < 0.005$  vs. same dose of EVs derived from an ADPKD-*PKD1*<sub>tr</sub> patient.

▢  $p < 0.05$  and ▨▢  $p < 0.005$  vs. 10  $\mu\text{g}/\text{mL}$  dose of EVs from same sample.

#  $p < 0.05$  and ##  $p < 0.005$  vs. 50  $\mu\text{g}/\text{mL}$  dose of EVs from same sample.

### 3 Discussion

Our aims for this study were to investigate the effects of urinary EV treatments on cystic renal epithelial cell proliferation. Due to the unintended cytotoxicity experienced by the cells in our experiment, however, we are unable to make any conclusions about the effect of the EV treatments on proliferation under normal conditions as intended. Instead, we can use this experimental setting to determine whether the EVs have a *protective* effect on cell survival under cytotoxic conditions. Similarly to our initial hypothesis, we predicted that the patient-derived EVs would have a stronger protective effect that increases survival of the cells, either by increasing proliferation (and thus ameliorating overall loss) or by increasing resistance to the cytotoxic effects. We based this prediction on the following observations: (a) renal epithelial cells with disease-causing variants in *PKD1* or *PKD2* have been shown to exhibit both of these behaviors (increased proliferation<sup>1</sup> and increased resistance to some cytotoxic treatments like cisplatin<sup>28</sup>); (b) because ADPKD patients only have a disease-causing variant in *one* allele of *PKD1* or *PKD2*, their renal epithelial cells still contain some levels of functional PC1 and PC2 from expression of the unaffected allele; and (c) treatment of healthy renal epithelial cells with EVs derived from *PKD1*-null renal epithelial cells has been shown to reduce PC1 levels in the healthy cells.<sup>20</sup> Therefore, if a reduction in functional polycystin levels results in increased renal epithelial cell proliferation and/or resistance to cytotoxic conditions, and treatment with EVs derived from ADPKD patients further reduces the levels of PC1 or PC2 in cystic cells, we would expect to see increased survival of cystic cells under cytotoxic conditions after treatment with patient-derived EVs.

Our results support this prediction. Treatment with ADPKD patient-derived urinary EVs at doses of 50 µg/mL and 100 µg/mL increased the relative-survival of cystic renal epithelial cells significantly more than treatment with EVs derived from a healthy individual, at almost every time-point. This effect was dose-dependent, as well: at all time-points, higher doses of patient-derived EVs increased relative-survival significantly more than lower doses. Doses of 100 µg/mL increased relative-survival more than doses of 50 µg/mL, which increased relative-survival more than doses of 10 µg/mL, which did not significantly increase relative-survival at all and even, in the single case of the ADPKD-*PKD1*<sub>tr</sub> patient-derived EVs at 24 hours, significantly *reduced* relative-survival ( $p = 0.02$ ). The reason for which this single reduction in relative-survival occurred is uncertain; because it seems to contradict both EV- and non-EV-based theories of ADPKD pathophysiology, this data point may not be reliable despite its statistical significance, and future experiments should determine its replicability. Despite this, the dose-dependency suggested by the other data points remains apparent. While a dose-dependent effect is not surprising, it is unclear why the treatment effect of patient-derived EVs is dose-dependent whereas the treatment effect of healthy individual-derived EVs seems not to be (or at least is not as strongly correlated with dose), especially given that treatment with

healthy individual-derived EVs did also increase relative-survival to some extent. One potential explanation is that, while both healthy and ADPKD EVs may promote cell proliferation, ADPKD EVs may additionally inhibit the activity of downstream signaling pathways which regulate proliferation – in other words, although both healthy and ADPKD EVs may “add gas to the tank”, ADPKD EVs may also cut the brake lines.

The treatment effect was also dependent on the patient from whom the EVs were derived, with 50 µg/mL and 100 µg/mL doses of EVs derived from an ADPKD-*PKD2*<sub>tr</sub> patient increasing relative-survival significantly more than the same doses of EVs derived from an ADPKD-*PKD1*<sub>tr</sub> patient, at both 24 and 48 hours after treatment. This is interesting, as we initially predicted that EVs derived from an ADPKD-*PKD1* patient would increase cell proliferation more than EVs derived from an ADPKD-*PKD2* patient. Whether this greater protective effect is specifically the result of the patient having a *PKD2* pathogenic variant, however, is unclear, especially considering that this would conflict with the reduced disease severity typically observed in ADPKD-*PKD2* patients compared to ADPKD-*PKD1* patients. Because only these two samples of patient-derived urinary EVs were used in this experiment, we cannot conclude with any certainty that the relative-survival differences observed were not instead the result of other differences in genetics and protein contents between the two EV samples. For example, while both patients’ pathogenic variants were truncating, the ADPKD-*PKD2*<sub>tr</sub> patient’s specific variant may have more substantially inhibited the incorporation of the affected polycystin into polycystin-complexes, or it may have more substantially inhibited the specific EV-biogenesis or EV-binding capabilities of the polycystin-complex, compared to the ADPKD-*PKD1*<sub>tr</sub> patient’s variant.

Overall, our results suggest that ADPKD patient-derived urinary EVs offer a protective effect against cytotoxicity to cystic renal epithelial cells, but this implication is by no means conclusive. Our experiment was not intended nor designed to assess protection against cytotoxicity, and much more strict control over the source of the cytotoxicity would be required to do so. We believe the cytotoxicity was most likely caused by the high amphotericin B concentration in the cell culture media, but, if we were to explicitly investigate the effects of EV treatments on amphotericin B cytotoxicity resistance, it would be more appropriate to implement several different doses of amphotericin B and assess the differences in cell survival after 72 hours. Instead, we aim to return to our initial hypothesis – based on proliferation under normal conditions rather than survival under cytotoxic conditions – in our future experiments. We plan to recalibrate our experimental conditions to ensure that the cells will grow over time rather than die, and re-perform the EV-treatment experiment under these conditions.

There are also several ways our experimental design could be improved in future work with respect to the EV treatments. First, our future experiments would benefit from the use of urinary EVs from more patients. Implementing treatments of EVs derived from additional ADPKD-*PKD1*<sub>tr</sub> and ADPKD-*PKD2*<sub>tr</sub> patients

would allow us to better control for unknown variations in the genetics and protein contents of EV samples and therefore obtain more conclusive evidence regarding whether the treatment effect is impacted by the EVs having a pathogenic variant in *PKD1* rather than *PKD2*. In addition, implementing treatments of EVs derived from ADPKD-*PKD1*<sub>nt</sub> and ADPKD-*PKD2*<sub>nt</sub> patients would also allow us to investigate whether the treatment effect is impacted by the EVs having a non-truncating mutation rather than a truncating mutation. Second, the selection of EV treatment doses could be better optimized: we chose to standardize doses across EV samples using total protein content to better compare our results to Ding et al.,<sup>20</sup> who did the same, but the cargo of EVs can vary considerably in total protein content, so this standardization method may be unreliable. Instead, future experiments could standardize doses in terms of number of EVs (measured by NTA) per cell or per mL of culture media. Third, the conclusions of future experiments could be strengthened by modifying the “untreated group” of cells (which were treated with PBS in this experiment) to instead be treated with non-functional EVs – EVs which could not be bound or taken in by the treated cells, such as EVs treated with neutralizing antibodies specific to EV membrane proteins like CD9 or the polycystin-complex proteins. This could allow for a more thorough investigation into whether it is truly the EVs which are changing the behavior of the treated cells, rather than, for example, other small proteins which could have been co-isolated with the EVs from the urine samples. Fourth, our EV isolation protocol could be better optimized to specifically isolate the EVs shed from proximal tubule epithelial cells which are heavily enriched for the polycystin proteins, rather than co-isolating EVs shed from all major segments of the nephron. The simplest way to accomplish this would be to add a step to the protocol – after the EVs are pelleted but before they are resuspended and filtered to remove potential bacterial/fungal contaminants – in which the EV pellet is resuspended, loaded onto a heavy-water 5–30% sucrose gradient, and again ultracentrifuged at 275,000×*g* overnight. Chen et al. (2013)<sup>24</sup> showed that this method is effective at separating the EVs into three distinct bands (that can be individually collected via fractionation), one of which is heavily enriched in PC1 and PC2 and likely consists of EVs shed from the proximal tubule. We were unable to implement this step due to a lack of the necessary instruments, but future work could benefit considerably from this added degree of EV isolation.

Future experiments would also benefit from the use of additional renal epithelial cell lines, in two primary ways. Firstly, the addition of a non-cystic cell line would allow us to better compare the impact of EV treatments in our cystic cell model to similar studies which more often use a non-cystic cell model, like that by Ding et al.<sup>20</sup> Secondly, the use of primary cell lines in place of the simian virus 40 (SV40)-immortalized cell line used in our experiment would allow for a more reasonable generalization of our results to the actual physiological conditions in ADPKD patients’ kidneys; SV40-immortalized cells grow much faster than primary cells and exhibit several differences in the expression of growth suppressors and in cell cycle regulation,<sup>29</sup>

making them potentially less representative of how cell proliferation would respond to treatments *in vivo*.

Finally, the results of future experiments could be interpreted more concretely if cell proliferation is measured in additional ways alongside XTT assays. XTT assays compare the metabolic activities of cell populations by measuring the colorimetric change resulting from the cells' reduction of tetrazolium salts to a soluble formazan product.<sup>30</sup> This serves as a useful way of comparing cell proliferation, as cell cultures with greater populations will exhibit higher overall metabolic activity and thus reduce the tetrazolium salts at a higher rate, but the assay is also subject to bias if treatments or culture conditions affect metabolic activity differently than they affect proliferation.<sup>30</sup> If future experiments additionally implemented, for example, fluorescent labels for proliferation markers measured by flow cytometry, we could more conclusively interpret whether changes in viability (measured by XTT assay) and changes in proliferation marker expression (measured by flow cytometry) reliably assess the changes in actual cell proliferation.

A future experiment with these changes implemented would therefore consist of primary cystic and non-cystic renal epithelial cells being treated with varying doses (e.g., 10,000 per seeded cell) of urinary EVs – derived from healthy individuals or from ADPKD patients, ideally with multiple treatment samples for each patient type listed in Table 1 – and then being cultured for 24, 48, or 72 hours under (non-cytotoxic) conditions which support net growth in untreated cells. Cell viability and expression of fluorescent-labeled proliferation markers would then be measured at each time point via XTT assay and flow cytometry, respectively. We would expect to obtain similar results from such an experiment as we obtained from our first EV-treatment experiment; i.e., we expect that patient-derived EVs would increase cell proliferation more than healthy individual-derived EVs, in a dose- and mutation-dependent manner. If we did obtain these results, it would give support to the EV-based theory proposed by Hogan and Ward<sup>13</sup> in a model closely resembling human ADPKD physiology, suggesting that mutations in *PKD1* and *PKD2* reduce the levels of functional polycystin-complexes in the membranes of renal epithelial cells and their EVs, which in turn hinders the ability of primary cilia to bind EVs and/or transport their cargo into the cell, thus inhibiting the EV-mediated signaling pathways that regulate cell proliferation (like the mTOR pathway or cAMP-promoting pathways<sup>1</sup>) and planar cell polarity (like the non-canonical Wnt signalling pathway<sup>13</sup>).

Such implications, however, would conflict with observed differences in the production of EVs by renal epithelial cells in ADPKD patients. It has been shown that ADPKD patients produce more urinary EVs (both by particle number and concentration of EV marker CD63) than healthy individuals.<sup>20</sup> If the polycystin-complex has primary roles both as a generator of new EVs and as a primary cilia-localized receiver of extracellular EVs, as Hogan and Ward<sup>13</sup> suggest, why do mutations in *PKD1* and *PKD2* which reduce the functionality of the polycystin-complex *increase* the quantity of EVs generated by renal epithelial cells? One potential explanation is that the increased excretion of urinary EVs in ADPKD patients is a result

of fewer EVs being successfully bound and received by primary cilia of renal epithelial cells due to loss of polycystin-complex functionality, rather than a result of increased biogenesis of EVs. Future work could test this by comparing the rate of EV-uptake by renal epithelial cells with a *PKD1* or *PKD2* mutation to that by non-cystic renal epithelial cells, as well as comparing their rates of uptake of ADPKD patient-/cell-derived EVs to their rates of uptake of healthy patient-/cell-derived EVs.

If true, an EV-based theory of ADPKD pathophysiology would have considerable implications for research in this field. EVs have already been implicated as potential biomarkers for monitoring the progression of ADPKD,<sup>23</sup> but an EV-centric mechanism for the genesis and expansion of kidney cysts would strongly implicate EVs as potential therapeutic targets as well. For example, if dysfunctional polycystin-complexes in the membranes of EVs prevent their binding and cargo-transfer to renal epithelial cells and thereby inhibit regulatory pathways for planar polarity and proliferation, then treatment of cystic renal epithelial cells with EVs containing functional polycystin-complexes (e.g., from healthy individuals or non-cystic cells) could help to ameliorate the signaling pathway disruptions and reduce cystic behavior. Huang et al. have very recently (March 2025) shown the potential in this theory, finding that ADPKD mice treated with urinary EVs derived from healthy mice exhibited “smaller kidney size, lower cyst index, and enhanced PC1 levels without affecting safety.”<sup>31</sup> Still, the exact mechanisms behind this observation are unclear, and it remains possible that the healthy EVs acted as deliverers of cyst-suppressing proteins in which the cystic cells were deficient, like PC1, rather than as signaling pathway facilitators replacing the dysfunctional EVs of the cystic cells.

The field of ADPKD research is a rapidly changing landscape, with new physiological mechanisms and therapeutic strategies being proposed and investigated every year. EV-based theories comprise a compelling subset of this latest research, showing great potential in the pursuit of understanding, monitoring, and treating the disease. Much of the interplay between disease-causing variants in *PKD1* or *PKD2* and the functionality of renal epithelial cell EVs remains uncertain, however, and a great deal more work must be dedicated to uncovering the truth of this relationship before the severity of ADPKD can be made a burden of the past.

## 4 Materials and methods

### 4.1 Cells and culture conditions

The cells used in all experiments were descended from cystic epithelial cells removed from a kidney cyst of an ADPKD-*PKD1*<sub>tr</sub> patient (see Table 2 for specific genetic information) and subsequently immortalized via transformation by simian virus 40 (SV40) large T antigen before being frozen in liquid nitrogen for storage. Before their use in our experiments, vials of these cells were removed from liquid nitrogen storage and rapidly thawed to minimize contact between thawed cells and their DMSO solution. The cells were then pelleted in 5 mL culture media per 1 mL DMSO suspension via centrifugation at 500 × g for 5 minutes, after which the media-diluted DMSO was removed and the pellet resuspended in 25 mL normal culture media. The cells were subsequently seeded in a T75 cell culture flask, where they were allowed to grow for at least 24 hours before use in any experiment. Cells were always cultured at 37 °C in 5% CO<sub>2</sub>.

Normal cell culture media consisted of Dulbecco's Modified Eagle Medium (DMEM) supplemented with fetal bovine serum (FBS) at 8% by volume, a penicillin-streptomycin solution to a final concentration of 100 I.U./mL penicillin and 100 µg/mL streptomycin, and amphotericin B to a final concentration of 2.50 µg/mL.

The composition of the cell culture media used to facilitate the various starvation conditions in the preliminary experiment was the same as normal cell culture media but with FBS concentrations varying from 0% to 10%. The cells cultured in media with 0.1% FBS exhibited the slowest positive growth over the 72-hour period (plotted without the other conditions for clarity in Figure 2a), so this FBS concentration was selected as the most appropriate starvation condition for our subsequent experiment implementing EV treatments. Due to concerns about potential contamination, the media concentration of amphotericin B was increased to 6.25 µg/mL at the start of the EV experiment. No other changes to the media composition were made.

Material	Gene	Nucleotide	Amino acid	Exon	Identifiers
Cell cultures	<i>PKD1</i> <i>PRKCSH</i>	c.6952del c.683C>T	p.Arg2318Alafs*23 p.Thr228Met	27 8	All cells used (see §4.1)
Urinary EVs	<i>PKD2</i>	c.1960C>T	p.Arg654*	9	ADPKD- <i>PKD2</i> <sub>tr</sub> patient “Patient 1”, Figure 1b & §4.3 “PKD2 truncating”, Figures 2–3 NTA sample, Figure 1c
Urinary EVs	<i>PKD1</i>	c.10321C>T	p.Gln3441*	33	ADPKD- <i>PKD1</i> <sub>tr</sub> patient “Patient 3”, Figure 1b & §4.3 “PKD1 truncating”, Figures 2–3

Table 2: Variants in ADPKD-associated genes possessed by cells and patients from whom urinary EVs were derived for this study. All variants are heterozygous. This data was collected by other members of the lab and by the Early PKD Observational Cohort Study (EPOC).

## 4.2 Isolation of urinary EVs

Extracellular vesicles were isolated from human urine by a process of differential centrifugation (see Figure 1a for a brief diagram of the protocol, and see Table 2 for specific genetic information for patient-derived samples). Urine was kept on ice and processed as soon as possible (< 60 minutes) after spontaneous void. Protease inhibitors were added to fresh urine as early as possible and prior to any centrifugation: 100  $\mu$ L each of 100  $\mu$ M aprotinin in H<sub>2</sub>O, 1 mM pepstatin A in DMSO, and 100 mM phenylmethylsulfonyl fluoride (PMSF) in isopropanol per 100 mL of urine. The urine was then transferred to 40 mL screw-top centrifuge tubes at equal volumes per tube and centrifuged at fixed angles at 4000 $\times g$  for 10 minutes at 4 °C. The top  $\frac{9}{10}$  of the supernatant was then collected from each tube. This supernatant was then divided into six clear 38.5 mL open-top ultracentrifuge tubes. The six tubes were grouped into three pairs, and the weights of tubes in each pair were adjusted (by adjusting volume of supernatant) until equal within 1  $\mu$ g. The tubes were then placed in a swinging-bucket rotor and spun at 10,000 $\times g$  for 10 minutes at 4 °C in an Optima™ XE ultracentrifuge. The process was then repeated – the top  $\frac{9}{10}$  of supernatant was collected and distributed into 6 new ultracentrifuge tubes which were adjusted for weight and then replaced into the swinging-bucket rotor – but this supernatant was spun at 150,000 $\times g$  for 60 minutes at 4 °C. This was sufficient to pellet the now-isolated urinary EVs; the supernatant was aspirated away and discarded, and the pellets were resuspended in a small amount of phosphate-buffered saline (PBS) (0.5-1 mL per 6 ultracentrifuge tubes).

Finally, the urinary EV solutions were sterilized by filtration. In a sterile biosafety cabinet, a 0.22  $\mu$ m-pore syringe filter was first primed (so as to prevent excess loss of EV protein) by the passage of 1 mL PBS, then 1 mL 0.1% (m/v) bovine serum albumin (BSA) in PBS, and then another 3 mL PBS. The EV isolation solutions were then drawn into a 3 mL syringe and passed through the filter into a sterile screw-top vial, which would thereafter only ever be re-opened in a sterile biosafety cabinet. A small volume of the isolation was aliquoted to a separate vial for later use in characterization experiments, so as to reduce the number of freeze-thaw cycles the samples experienced prior to use in the EV experiment. The isolations were frozen at –80 °C until their use.

## 4.3 Characterization of isolated urinary EVs

Total protein content in the samples of isolated urinary EVs was assayed using a Thermo Scientific™ Pierce™ BCA protein assay kit (cat. 23225). For each sample, 15  $\mu$ L of EVs and 1.5  $\mu$ L of 10% (m/v) sodium dodecyl sulfate (SDS) in ultrapure water were added to 58.5  $\mu$ L of PBS and then heated at 70 °C for 10 minutes in order to lyse the vesicles, after which 25  $\mu$ L of the solution (now a 1:5 dilution of the EV isolation sample) was added to each of three replicate wells in a 96-well plate. The same volumes of known-concentration BSA

protein standards (0–2000 µg/mL) were added across eight wells to allow for generation of a standard curve, and 200 µL of the kit’s working reagent was lastly added to each well containing sample or standard (or PBS to serve as blank). The plate was incubated for 30 minutes at 37 °C and then the wells’ absorbances at 562 nm were read on a microplate scanner, allowing the total protein concentration in each sample of isolated EVs to be calculated. These protein concentrations were used to define the doses used in the EV-treatment experiment and to control the amount of protein loaded onto individual wells in the subsequent gel electrophoresis and western blot experiments.

Detection of the tetraspanin EV marker CD9 in the patient EV isolation samples was accomplished through gel electrophoresis and western blot procedures. This experiment was performed using three EV isolation samples, each derived from the urine of a different ADPKD patient (Patients 1, 2, and 3; see Table 2). For the Patient 1 sample, 20 µg of sample protein (11.1 µL) was diluted in 7.3 µL of PBS. For the Patient 2 sample, 6.5 µg of sample protein (8.3 µL) was diluted in 10.1 µL of PBS. For the Patient 3 sample, 20 µg of sample protein (16.3 µL) was added to 2.1 µL of PBS. To each of these three diluted samples, 6.1 µL of 4X Invitrogen™ NuPAGE™ LDS Sample Buffer (cat. NP0007) was added, giving a final volume of 24.5 µL for each of these prepared samples. No reducing agent was added (nor antioxidant during the running and transfer stages), because the epitope recognized by antibodies to tetraspanins like CD9 usually relies on several disulfide bonds for recognition, and so blotting for CD9 requires nonreducing electrophoresis.<sup>32</sup>

Each of the three western blot samples was heated at 70 °C for 10 minutes and then its entire 24.5 µL volume was added to its own well of a 4–12% 1.5 mm Invitrogen™ NuPAGE™ Bis-Tris mini protein gel (cat. NP0335BOX) alongside a well containing 5 µL of broad range Bio-Rad Prestained SDS-PAGE Standards (cat. 161-0318) diluted in 6.1 µL LDS and 13.4 µL of PBS. The gel was run in MOPS running buffer at 60 V for 30 minutes and then at 120 V until the dye reached the gel foot. Protein bands were transferred to a methanol-activated PVDF membrane in transfer buffer at 30 V for one hour. The membrane was next blocked in a mixture of 0.1% (by volume) Tween 20 in Tris-buffered saline (TBST) plus 5% BSA for 60 minutes at 4 °C. A 1:1000 dilution of Invitrogen CD9 Recombinant Rabbit Monoclonal Antibody (cat. MA5-35212) in 1% BSA in Tris-buffered saline (TBS) was made and added to the membrane after removal of the blocking buffer, and the membrane was allowed to gently rock in the solution overnight at 4 °C. The membrane was then washed in TBST for 5, 10, and 15 minutes successively before being allowed to rock in a 1:5000 dilution of goat anti-rabbit IgG secondary antibody in TBS for 90 minutes in the dark. The membrane was washed again in TBST for 5, 10, and 15 minutes successively, and finally washed once in TBS for 5 minutes before being immediately scanned on a LiCOR Odyssey infrared-spectrum scanner for fluorescence (Figure 1b). The western blot procedure for detecting the second tetraspanin EV marker CD81 in three other isolated urinary EV samples was very similar, but this was performed by other members of

the lab.

Nanoparticle tracking analysis (NTA) was performed under guided supervision by trained technicians at The University of Chicago Biophysics Core Facility on a NanoSight NS300 instrument using several isolated urinary EV samples to ensure the majority of particles were within the expected diameter range of EVs (one representative result is shown in Figure 1c). The instrument was thoroughly cleaned before and between each use. To collect measurements of particle quantity and size distribution, small volumes of each sample were passed through capillary tubes at a constant rate while the instrument recorded videos at the nanometer-scale. For each sample, five minute-long videos were recorded and analyzed automatically for particle diameters and frequencies as well as standard error estimations.

Samples were prepared for negative stain transmission electron microscopy imaging by a member of the lab other than myself, after which trained technicians at The University of Chicago Advanced Electron Microscopy Core Facility captured the images presented in Figure 1d without my own involvement. I cannot speak to the specific protocol used, but, generally, the procedure involves first fixing the EVs at room temperature with 0.1% paraformaldehyde in PBS, pipeting 10  $\mu$ L of each EV sample onto Parafilm, transferring the samples onto a carbon-coated copper grid, incubating the grid and samples in 10  $\mu$ L of 2% uranyl acetate, and finally imaging the grid.<sup>33</sup> Further details can be found in the protocol described by Cizmar and Yuana (2017).<sup>33</sup>

#### 4.4 Determination of starvation conditions

Proper starvation conditions in terms of FBS concentration in growth media were determined via a very similar 72-hour population growth experiment as the primary EV-treatment experiment around which this paper is focused. Cells which had grown to moderate (around 70%) confluence in normal culture media were first counted. This entailed removing the media from the flask of adherent cells, gently washing once with 10 mL of PBS, adding 3 mL of 0.0625% trypsin-EDTA solution on top of the cells for 4 minutes to detach them from the flask, adding 9 mL of new, FBS-free culture media to the cell-trypsin suspension and homogenizing, adding a small volume (around 100  $\mu$ L) of this suspension to a vial containing an equal volume of trypan blue, and counting the cells in this solution using an Invitrogen Countess 3 Automated Cell Counter while the larger volume of homogenized cells was gently shaken to prevent re-adherence of cells to the flask walls.

Once the cell count and concentration was determined, an appropriate dilution of the suspension was made such that a volume of 200  $\mu$ L (the recommended volume per well of a 96-well plate) would contain approximately  $1 \times 10^4$  cells, and this volume was added to each of 144 wells across 4 plates (one plate per time-point, 36 wells per plate). In each of the three plates besides that for time-point 0, the wells were split

into 6 groups of 6 replicate-wells each, with each group corresponding to an FBS-concentration treatment (0%, 0.1%, 0.5%, 1%, 2%, or 10%). Cell-free media was added to an additional 6 wells per plate to provide a blank for the later XTT assays. FBS was added to each well of the three later-time-point plates according to its treatment group, after which an XTT assay was performed on the time-zero plate which had not been treated with any FBS (the initiation of the XTT assay did not actually occur until 2 hours after FBS was added to the other plates due to time constraints, which is why the data in Figure 2a begins at 2 hours rather than 0 hours; this discrepancy was mitigated in the later EV-focused experiment). Subsequent XTT assays were initiated at 24, 48, and 72 hours after the addition of FBS to the wells. Each plate was discarded after having left the sterility of the culture room for XTT measurement.

#### 4.5 Treatment of cells with urinary EVs

The procedure for the EV-based experiment was the same as that for the above-described FBS-based experiment, except for the following differences: the cell culture media was slightly different (though perhaps adversely so – see Section 2.2); ten treatment groups were implemented rather than six; the treatment groups (see below) were divided based on the individual from whom the urinary EVs were derived and on the dose of EVs used, rather than on the concentration of FBS, of which all wells' media contained 0.1%; EVs were diluted into 20  $\mu$ L volumes (with concentrations corresponding to dose) to be added to each well rather than directly adding different volumes of EVs onto wells, so that each well's total volume was the same (200  $\mu$ L) regardless of treatment; and the XTT assay for the time-zero plate was initiated immediately after treatment with EVs rather than two hours after.

Treatments were the same for each time-point (besides the length of incubation time), and consisted of one of the following added to each well:

- Treatment group 1 (untreated) — 20  $\mu$ L of PBS
- Treatment groups 2-4 — 20  $\mu$ L of urinary EVs, derived from a healthy individual (Figure 1d), suspended in PBS at a dose of either 10, 50, or 100  $\mu$ g of protein per mL of final well volume
- Treatment groups 5-7 — 20  $\mu$ L of urinary EVs, derived from an ADPKD-*PKD2*<sub>tr</sub> patient (see Table 2), suspended in PBS at a dose of either 10, 50, or 100  $\mu$ g of protein per mL of final well volume
- Treatment groups 8-10 — 20  $\mu$ L of urinary EVs, derived from an ADPKD-*PKD1*<sub>tr</sub> patient (see Table 2), suspended in PBS at a dose of either 10, 50, or 100  $\mu$ g of protein per mL of final well volume

#### 4.6 XTT assays

XTT assays for cell viability were performed to measure relative changes in cell populations (not absolute populations, as no standard assay for calibration was implemented) at each time point of the two growth

experiments described above. The assays were carried out using a TACS<sup>®</sup> XTT Cell Proliferation Assay kit (cat. 4891-025-K), with no deviations from the manufacturer's instructions found at <https://resourcesrndsystems.com/pdfs/datasheets/4891-025-k.pdf?v=20250420>.

## 4.7 Statistical Analyses

The results of the XTT assays are shown in Figure 2 in terms of “mean fold change” and in Figure 3 in terms of “mean relative-survival”. These values were respectively calculated as

$$\bar{F}_{gt} = \frac{\overline{\text{Abs}}_{gt}}{\text{Abs}_0} = \left( \frac{\frac{1}{R} \sum_{r=1}^R \text{Abs}_{gt,r}}{\frac{1}{R_0} \sum_{r=1}^{R_0} \text{Abs}_{0,r}} \right) \quad (1)$$

$$\bar{S}_{gt} = \frac{\overline{\text{Abs}}_{gt}}{\text{Abs}_{ut}} \cdot 100\% = \left( \frac{\sum_{r=1}^R \text{Abs}_{gt,r}}{\sum_{r=1}^R \text{Abs}_{ut,r}} \right) \cdot 100\% \quad (2)$$

with variables as defined in Table 3.

Variable	Definition
$F_{gt}$	Fold change of cells in treatment group $g$ at time-point $t$
$S_{gt}$	Relative-survival of cells in treatment group $g$ at time-point $t$
$\text{Abs}_{gt,r}$	Corrected-absorbance measured in replicate $r$ of cells in treatment group $g$ at time-point $t$
$\text{Abs}_{0,r}$	Corrected-absorbance measured in replicate $r$ of cells at hour 0
$\text{Abs}_{ut,r}$	Corrected-absorbance measured in replicate $r$ of untreated cells at time-point $t$
$R$	Total number of replicates per treatment group per time-point (not including hour 0) $R = 6$ for all XTT assays performed
$R_0$	Total number of replicates at hour 0 $R_0 = 36$ for the FBS experiment (Figure 2a); $R_0 = 60$ for the EV experiment (Figure 2b)
$\bar{X}$	Sample mean of variable $X$

Table 3: Definitions of variables used in all equations. In the last definition,  $X$  is a placeholder for any of the above-listed variables.

Error bars in Figures 2 and 3 represent  $\pm 1$  standard error. Because the calculations of both fold change and relative-survival involved dividing one mean absorbance by another, and visual assessment of the histograms of absorbance values suggested they did not follow an explicit probability distribution, standard errors were estimated via bootstrapping: the mean relative-survival and mean fold change were calculated for each of 10,000 resamples with replacement of the corrected-absorbance data, and the standard deviations of these two bootstrapped sampling distributions were used as the standard errors for relative-survival and fold change, respectively.

Because the relative-survival values also did not follow a normal (or otherwise explicit) probability distribution, the  $p$ -values for all statistical tests (labeled in Figure 3) were computed via nonparametric Mann–Whitney  $U$  tests. Relative-survival comparisons between cells treated with ADPKD patient-derived urinary EVs and cells treated with healthy individual-derived urinary EVs were performed as one-sided tests, whereas relative-survival comparisons between cells treated with ADPKD- $PKD1_{\text{tr}}$  patient-derived EVs and cells treated with ADPKD- $PKD2_{\text{tr}}$  patient-derived EVs were performed as two-sided tests.

Data manipulation, statistical analyses, and plot generation were performed in the R programming language (version 4.4.2)<sup>34</sup> using the packages listed in Table 4. The code for these analyses and plots, as well as the raw data from the XTT assays, is available at <https://github.com/c-lozano/Thesis-Data>.

Package name	Version	Maintainer	Ref.
knitr	1.49	Yihui Xie – <a href="mailto:xie@yihui.name">xie@yihui.name</a>	<a href="#">35,36,37</a>
pacman	0.5.1	Tyler Rinker – <a href="mailto:tyler.rinker@gmail.com">tyler.rinker@gmail.com</a>	<a href="#">38,39</a>
patchwork	1.3.0	Thomas Lin Pedersen – <a href="mailto:thomaspedersen@posit.co">thomaspedersen@posit.co</a>	<a href="#">40</a>
ggplot2	3.5.1	Thomas Lin Pedersen – <a href="mailto:thomas.pedersen@posit.co">thomas.pedersen@posit.co</a>	<a href="#">41,42</a>
tibble	3.2.1	Kirill Müller – <a href="mailto:kirill@cynkra.com">kirill@cynkra.com</a>	<a href="#">43</a>
tidyr	1.3.1	Hadley Wickham – <a href="mailto:hadley@posit.co">hadley@posit.co</a>	<a href="#">44</a>
readr	2.1.5	Jennifer Bryan – <a href="mailto:jenny@posit.co">jenny@posit.co</a>	<a href="#">45</a>
dplyr	1.1.4	Hadley Wickham – <a href="mailto:hadley@posit.co">hadley@posit.co</a>	<a href="#">46</a>
stringr	1.5.1	Hadley Wickham – <a href="mailto:hadley@posit.co">hadley@posit.co</a>	<a href="#">47</a>

Table 4: R packages used for the manipulation of data, generation of plots, and statistical analyses.

## 5 Acknowledgments

I would like to thank Dr. Arlene Chapman, Dr. Peili Chen, and Dr. Oliver Wessely for their constant advice and help throughout the undertaking of this project, as well as Dr. Brandon Faubert and Dr. Joseph Franses for providing me feedback on this thesis. Finally, I would like to thank the Jack Kent Cooke Foundation for funding my work during the summer of 2024.

## References

1. Niloofar Nobakht, Ramy M. Hanna, Maha Al-Baghdadi, Khalid Mohammed Ameen, Farid Arman, Ehsan Nobakht, Mohammad Kamgar, and Anjay Rastogi. Advances in Autosomal Dominant Polycystic Kidney Disease: A Clinical Review. *Kidney Medicine*, 2(2):196–208, March 2020. ISSN 2590-0595. doi: 10.1016/j.xkme.2019.11.009. URL <https://www.sciencedirect.com/science/article/pii/S2590059520300285>.
2. Fouad T. Chebib and Vicente E. Torres. Autosomal Dominant Polycystic Kidney Disease: Core Curriculum 2016. *American Journal of Kidney Diseases*, 67(5):792–810, May 2016. ISSN 0272-6386. doi: 10.1053/j.ajkd.2015.07.037. URL <https://www.sciencedirect.com/science/article/pii/S0272638615012160>.
3. Peter Igarashi, Stefan Somlo, and Feature Editor. Genetics and Pathogenesis of Polycystic Kidney Disease. *Journal of the American Society of Nephrology*, 13(9):2384, September 2002. ISSN 1046-6673. doi: 10.1097/01.ASN.0000028643.17901.42. URL [https://journals.lww.com/jasn/fulltext/2002/09000/genetics\\_and\\_pathogenesis\\_of\\_polycystic\\_kidney.22.aspx](https://journals.lww.com/jasn/fulltext/2002/09000/genetics_and_pathogenesis_of_polycystic_kidney.22.aspx).
4. G. M. Fick, A. M. Johnson, J. D. Strain, W. J. Kimberling, S. Kumar, M. L. Manco-Johnson, I. T. Duley, and P. A. Gabow. Characteristics of very early onset autosomal dominant polycystic kidney disease. *Journal of the American Society of Nephrology*, 3(12):1863, June 1993. ISSN 1046-6673. doi: 10.1681/ASN.V3121863. URL [https://journals.lww.com/JASN/abstract/1993/06000/Characteristics\\_of\\_very\\_early\\_onset\\_autosomal.3.aspx](https://journals.lww.com/JASN/abstract/1993/06000/Characteristics_of_very_early_onset_autosomal.3.aspx).
5. Irina M. Sanchis, Shehbaz Shukoor, Maria V. Irazabal, Charles D. Madsen, Fouad T. Chebib, Marie C. Hogan, Ziad El-Zoghby, Peter C. Harris, John Huston, Robert D. Brown, and Vicente E. Torres. Presymptomatic Screening for Intracranial Aneurysms in Patients with Autosomal Dominant Polycystic Kidney Disease. *Clinical Journal of the American Society of Nephrology : CJASN*, 14(8):1151–1160, August 2019. ISSN 1555-9041. doi: 10.2215/CJN.14691218. URL <https://www.ncbi.nlm.nih.gov/pmc/articles/PMC6682820/>.
6. Matthew Taylor, Ann M. Johnson, Maryellyn Tison, Pamela Fain, and Robert W. Schrier. Earlier Diagnosis of Autosomal Dominant Polycystic Kidney Disease: Importance of Family History and Implications for Cardiovascular and Renal Complications. *American Journal of Kidney Diseases*, 46(3):415–423, September 2005. ISSN 0272-6386. doi: 10.1053/j.ajkd.2005.05.029. URL <https://www.sciencedirect.com/science/article/pii/S0272638605007821>.
7. Carsten Bergmann. Ciliopathies. *European Journal of Pediatrics*, 171(9):1285–1300, September 2012. ISSN 1432-1076. doi: 10.1007/s00431-011-1553-z. URL <https://doi.org/10.1007/s00431-011-1553-z>.
8. Vicente E Torres, Peter C Harris, and Yves Pirson. Autosomal dominant polycystic kidney disease. *The Lancet*, 369(9569):1287–1301, April 2007. ISSN 0140-6736. doi: 10.1016/S0140-6736(07)60601-1. URL <https://www.sciencedirect.com/science/article/pii/S0140673607606011>.
9. Arlene B. Chapman, Olivier Devuyst, Kai-Uwe Eckardt, Ron T. Gansevoort, Tess Harris, Shigeo Horie, Bertram L. Kasiske, Dwight Odland, York P. Pei, Ronald D. Perrone, Yves Pirson, Robert W. Schrier, Roser Torra, Vicente E. Torres, Terry Watnick, and David C. Wheeler. Autosomal Dominant Polycystic Kidney Disease (ADPKD): Executive Summary from a Kidney Disease: Improving Global Outcomes (KDIGO) Controversies Conference. *Kidney International*, 88(1):17–27, July 2015. ISSN 0085-2538. doi: 10.1038/ki.2015.59. URL <https://www.ncbi.nlm.nih.gov/pmc/articles/PMC4913350/>.
10. Christina M. Heyer, Jamie L. Sundsbak, Kaleab Z. Abebe, Arlene B. Chapman, Vicente E. Torres, Jared J. Grantham, Kyongtae T. Bae, Robert W. Schrier, Ronald D. Perrone, William E. Braun, Theodore I. Steinman, Michal Mrug, Alan S. L. Yu, Godela Brosnahan, Katharina Hopp, Maria V. Irazabal, William M. Bennett, Michael F. Flessner, Charity G. Moore, Douglas Landsittel, Peter C. Harris, and for the HALT PKD and CRISP Investigators. Predicted Mutation Strength of Nontruncating PKD1 Mutations Aids Genotype-Phenotype Correlations in Autosomal Dominant Polycystic Kidney

- Disease. *Journal of the American Society of Nephrology*, 27(9):2872, September 2016. ISSN 1046-6673. doi: 10.1681/ASN.2015050583. URL [https://journals.lww.com/jasn/fulltext/2016/09000/predicted\\_mutation\\_strength\\_of\\_nontruncating\\_pkd1.32.aspx](https://journals.lww.com/jasn/fulltext/2016/09000/predicted_mutation_strength_of_nontruncating_pkd1.32.aspx).
11. Emilie Cornec-Le Gall, Marie-Pierre Audrézet, Jian-Min Chen, Maryvonne Hourmant, Marie-Pascale Morin, Régine Perrichot, Christophe Charasse, Bassem Whebe, Eric Renaudineau, Philippe Jousset, Marie-Paule Guillodo, Anne Grall-Jezequel, Philippe Saliou, Claude Férec, and Yannick Le Meur. Type of PKD1 Mutation Influences Renal Outcome in ADPKD. *Journal of the American Society of Nephrology*, 24(6):1006, June 2013. ISSN 1046-6673. doi: 10.1681/ASN.2012070650. URL [https://journals.lww.com/jasn/abstract/2013/06000/type\\_of\\_pkd1\\_mutation\\_influences\\_renal\\_outcome\\_in.20.aspx](https://journals.lww.com/jasn/abstract/2013/06000/type_of_pkd1_mutation_influences_renal_outcome_in.20.aspx).
  12. Vicente E. Torres, Curie Ahn, Thijs R. M. Barten, Godela Brosnahan, Melissa A. Cadnapaphornchai, Arlene B. Chapman, Emilie Cornec-Le Gall, Joost P. H. Drenth, Ron T. Gansevoort, Peter C. Harris, Tess Harris, Shigeo Horie, Max C. Liebau, Michele Liew, Andrew J. Mallett, Changlin Mei, Djalila Mekahli, Dwight Odland, Albert C. M. Ong, Luiz F. Onuchic, York P-C. Pei, Ronald D. Perrone, Gopala K. Rangan, Brian Rayner, Roser Torra, Ethan M. Balk, Craig E. Gordon, Amy Earley, Reem A. Mustafa, and Olivier Devuyst. KDIGO 2025 clinical practice guideline for the evaluation, management, and treatment of autosomal dominant polycystic kidney disease (ADPKD): executive summary. *Kidney International*, 107(2):234–254, February 2025. ISSN 0085-2538. doi: 10.1016/j.kint.2024.07.010. URL <https://www.sciencedirect.com/science/article/pii/S0085253824004812>.
  13. Marie C. Hogan and Christopher J. Ward. An extracellular vesicle based hypothesis for the genesis of the polycystic kidney diseases. *Extracellular Vesicle*, 4:100048, December 2024. ISSN 2773-0417. doi: 10.1016/j.vesic.2024.100048. URL <https://www.sciencedirect.com/science/article/pii/S2773041724000155>.
  14. Wendy A. Lea, Thomas Winklhofer, Lesya Zelenchuk, Madhulika Sharma, Jessica Rossol-Allison, Timothy A. Fields, Gail Reif, James P. Calvet, Jason L. Bakeberg, Darren P. Wallace, and Christopher J. Ward. Polycystin-1 Interacting Protein-1 (CU062) Interacts with the Ectodomain of Polycystin-1 (PC1). *Cells*, 12(17):2166, January 2023. ISSN 2073-4409. doi: 10.3390/cells12172166. URL <https://www.mdpi.com/2073-4409/12/17/2166>. Number: 17 Publisher: Multidisciplinary Digital Publishing Institute.
  15. Elisa A. Nigro and Alessandra Boletta. Role of the polycystins as mechanosensors of extracellular stiffness. *American Journal of Physiology-Renal Physiology*, 320(5):F693–F705, May 2021. ISSN 1931-857X. doi: 10.1152/ajprenal.00545.2020. URL <https://journals.physiology.org/doi/full/10.1152/ajprenal.00545.2020>. Publisher: American Physiological Society.
  16. Jana Reiterová and Vladimír Tesař. Autosomal Dominant Polycystic Kidney Disease: From Pathophysiology of Cystogenesis to Advances in the Treatment. *International Journal of Molecular Sciences*, 23(6):3317, January 2022. ISSN 1422-0067. doi: 10.3390/ijms23063317. URL <https://www.mdpi.com/1422-0067/23/6/3317>. Number: 6 Publisher: Multidisciplinary Digital Publishing Institute.
  17. Feng Qian, Terry J Watnick, Luiz F Onuchic, and Gregory G Germino. The Molecular Basis of Focal Cyst Formation in Human Autosomal Dominant Polycystic Kidney Disease Type I. *Cell*, 87(6):979–987, December 1996. ISSN 0092-8674. doi: 10.1016/S0092-8674(00)81793-6. URL <https://www.sciencedirect.com/science/article/pii/S0092867400817936>.
  18. Irma S. Lantinga-van Leeuwen, Johannes G. Dauwerse, Hans J. Baelde, Wouter N. Leonhard, Annemieke van de Wal, Christopher J. Ward, Sjef Verbeek, Marco C. DeRuiter, Martijn H. Breuning, Emile de Heer, and Dorien J.M. Peters. Lowering of Pkd1 expression is sufficient to cause polycystic kidney disease. *Human Molecular Genetics*, 13(24):3069–3077, December 2004. ISSN 0964-6906. doi: 10.1093/hmg/ddh336. URL <https://doi.org/10.1093/hmg/ddh336>.
  19. María Yáñez-Mó, Pia R.-M. Siljander, Zoraida Andreu, Apolonija Bedina Zavec, Francesc E. Borràs, Edit I. Buzas, Krisztina Buzas, Enriqueta Casal, Francesco Cappello, Joana Carvalho, Eva Colás, Anabela Cordeiro-da Silva, Stefano Fais, Juan M. Falcon-Perez, Irene M. Ghobrial, Bernd Giebel, Mario

- Gimona, Michael Graner, Ihsan Gursel, Mayda Gursel, Niels H. H. Heegaard, An Hendrix, Peter Kierulf, Katsutoshi Kokubun, Maja Kosanovic, Veronika Kralj-Iglic, Eva-Maria Krämer-Albers, Saara Laitinen, Cecilia Lässer, Thomas Lener, Erzsébet Ligeti, Aija Linē, Georg Lipps, Alicia Llorente, Jan Lötvall, Mateja Manček-Keber, Antonio Marcilla, Maria Mittelbrunn, Irina Nazarenko, Esther N.M. Nolte-'t Hoen, Tuula A. Nyman, Lorraine O'Driscoll, Mireia Olivan, Carla Oliveira, Éva Pállinger, Hernando A. del Portillo, Jaume Reventós, Marina Rigau, Eva Rohde, Marei Sammar, Francisco Sánchez-Madrid, N. Santarém, Katharina Schallmoser, Marie Stampe Ostenfeld, Willem Stoorvogel, Roman Stukelj, Susanne G. Van der Grein, M. Helena Vasconcelos, Marca H. M. Wauben, and Olivier De Wever. Biological properties of extracellular vesicles and their physiological functions. *Journal of Extracellular Vesicles*, 4(1):27066, 2015. doi: <https://doi.org/10.3402/jev.v4.27066>. URL <https://isevjournals.onlinelibrary.wiley.com/doi/abs/10.3402/jev.v4.27066>. eprint: <https://isevjournals.onlinelibrary.wiley.com/doi/pdf/10.3402/jev.v4.27066>.
20. Hao Ding, Linda Xiaoyan Li, Peter C. Harris, Junwei Yang, and Xiaogang Li. Extracellular vesicles and exosomes generated from cystic renal epithelial cells promote cyst growth in autosomal dominant polycystic kidney disease. *Nature Communications*, 12(1):4548, July 2021. ISSN 2041-1723. doi: 10.1038/s41467-021-24799-x. URL <https://www.nature.com/articles/s41467-021-24799-x>. Publisher: Nature Publishing Group.
  21. Theresa L. Whiteside. Chapter Four - Tumor-Derived Exosomes and Their Role in Cancer Progression. In Gregory S. Makowski, editor, *Advances in Clinical Chemistry*, volume 74, pages 103–141. Elsevier, January 2016. doi: 10.1016/bs.acc.2015.12.005. URL <https://www.sciencedirect.com/science/article/pii/S0065242315300056>.
  22. George K. Tofaris. A Critical Assessment of Exosomes in the Pathogenesis and Stratification of Parkinson's Disease. *Journal of Parkinson's Disease*, 7(4):569, November 2017. doi: 10.3233/JPD-171176. URL <https://pmc.ncbi.nlm.nih.gov/articles/PMC5676982/>.
  23. Marie C. Hogan, Jason L. Bakeberg, Vladimir G. Gainullin, Maria V. Irazabal, Amber J. Harmon, John C. Lieske, M. Cristine Charlesworth, Kenneth L. Johnson, Benjamin J. Madden, Roman M. Zenka, Daniel J. McCormick, Jamie L. Sundsbak, Christina M. Heyer, Vicente E. Torres, Peter C. Harris, and Christopher J. Ward. Identification of Biomarkers for PKD1 Using Urinary Exosomes. *Journal of the American Society of Nephrology*, 26(7):1661, July 2015. ISSN 1046-6673. doi: 10.1681/ASN.2014040354. URL [https://journals.lww.com/jasn/fulltext/2015/07000/identification\\_of\\_biomarkers\\_for\\_pkd1\\_using\\_21.aspx](https://journals.lww.com/jasn/fulltext/2015/07000/identification_of_biomarkers_for_pkd1_using_21.aspx).
  24. Christopher Y. Chen, Marie C. Hogan, and Christopher J. Ward. Purification of Exosome-like Vesicles from Urine. *Methods in enzymology*, 524:225, 2013. doi: 10.1016/B978-0-12-397945-2.00013-5. URL <https://www.ncbi.nlm.nih.gov/pmc/articles/PMC4028690/>. Publisher: NIH Public Access.
  25. Charles J. Blijdorp, Omar A. Z. Tutakhel, Thomas A. Hartjes, Thierry P. P. van den Bosch, Martijn H. van Heugten, Juan Pablo Rigalli, Rob Willemsen, Usha M. Musterd-Bhaggoe, Eric R. Barros, Roger Carles-Fontana, Cristian A. Carvajal, Onno J. Arntz, Fons A. J. van de Loo, Guido Jenster, Marian C. Clahsen-van Groningen, Cathy A. Cuevas, David Severs, Robert A. Fenton, Martin E. van Royen, Joost G. J. Hoenderop, René J. M. Bindels, and Ewout J. Hoorn. Comparing Approaches to Normalize, Quantify, and Characterize Urinary Extracellular Vesicles. *Journal of the American Society of Nephrology*, 32(5):1210, May 2021. ISSN 1046-6673. doi: 10.1681/ASN.2020081142. URL [https://journals.lww.com/jasn/fulltext/2021/05000/comparing\\_approaches\\_to\\_normalize,\\_quantify,\\_and\\_23.aspx](https://journals.lww.com/jasn/fulltext/2021/05000/comparing_approaches_to_normalize,_quantify,_and_23.aspx).
  26. Yé Fan, Cédric Pionneau, Federico Cocozza, Pierre-Yves Boëlle, Solenne Chardonnet, Stéphanie Charrin, Clotilde Théry, Pascale Zimmermann, and Eric Rubinstein. Differential proteomics argues against a general role for CD9, CD81 or CD63 in the sorting of proteins into extracellular vesicles. *Journal of Extracellular Vesicles*, 12(8):12352, 2023. ISSN 2001-3078. doi: 10.1002/jev2.12352. URL <https://onlinelibrary.wiley.com/doi/abs/10.1002/jev2.12352>. eprint: <https://onlinelibrary.wiley.com/doi/pdf/10.1002/jev2.12352>.

27. Despina E. Varlam, Mustafa M. Siddiq, Lance A. Parton, and Holger Rüssmann. Apoptosis Contributes to Amphotericin B- Induced Nephrotoxicity. *Antimicrobial Agents and Chemotherapy*, 45(3):679–685, March 2001. doi: 10.1128/aac.45.3.679-685.2001. URL <https://journals.asm.org/doi/full/10.1128/aac.45.3.679-685.2001>. Publisher: American Society for Microbiology.
28. Sayanthooran Saravanabavan and Gopala K. Rangan. Kidney Cyst Lining Epithelial Cells Are Resistant to Low-Dose Cisplatin-Induced DNA Damage in a Preclinical Model of Autosomal Dominant Polycystic Kidney Disease. *International Journal of Molecular Sciences*, 23(20):12547, January 2022. ISSN 1422-0067. doi: 10.3390/ijms232012547. URL <https://www.mdpi.com/1422-0067/23/20/12547>. Number: 20 Publisher: Multidisciplinary Digital Publishing Institute.
29. Krishna K. Jha, Satnam Banga, Vaseem Palejwala, and Harvey L. Ozer. SV40-Mediated Immortalization. *Experimental Cell Research*, 245(1):1–7, November 1998. ISSN 0014-4827. doi: 10.1006/excr.1998.4272. URL <https://www.sciencedirect.com/science/article/pii/S0014482798942720>.
30. Kamalendra Yadav, Nitin Singhal, Vikas Rishi, and Hariom Yadav. Cell Proliferation Assays. In *eLS*. John Wiley & Sons, Ltd, 2014. ISBN 978-0-470-01590-2. doi: 10.1002/9780470015902.a0002566. eprint: <https://onlinelibrary.wiley.com/doi/pdf/10.1002/9780470015902.a0002566>.
31. Yi Huang, Ali Osouli, Hui Li, Megan Dusaney, Jessica Pham, Valeria Mancino, Taranatee Khan, Baishali Chaudhuri, Nuria M. Pastor-Soler, Kenneth R. Hallows, and Eun Ji Chung. Therapeutic potential of urinary extracellular vesicles in delivering functional proteins and modulating gene expression for genetic kidney disease. *Biomaterials*, 321:123296, October 2025. ISSN 0142-9612. doi: 10.1016/j.biomaterials.2025.123296. URL <https://www.sciencedirect.com/science/article/pii/S0142961225002157>.
32. Emma J. K. Kowal, Dmitry Ter-Ovanesyan, Aviv Regev, and George M. Church. Extracellular Vesicle Isolation and Analysis by Western Blotting. In Winston Patrick Kuo and Shidong Jia, editors, *Extracellular Vesicles: Methods and Protocols*, pages 143–152. Springer, New York, NY, 2017. ISBN 978-1-4939-7253-1. doi: 10.1007/978-1-4939-7253-1\_12. URL [https://doi.org/10.1007/978-1-4939-7253-1\\_12](https://doi.org/10.1007/978-1-4939-7253-1_12).
33. Petr Cizmar and Yuana Yuana. Detection and Characterization of Extracellular Vesicles by Transmission and Cryo-Transmission Electron Microscopy. In Winston Patrick Kuo and Shidong Jia, editors, *Extracellular Vesicles: Methods and Protocols*, pages 221–232. Springer, New York, NY, 2017. ISBN 978-1-4939-7253-1. doi: 10.1007/978-1-4939-7253-1\_18. URL [https://doi.org/10.1007/978-1-4939-7253-1\\_18](https://doi.org/10.1007/978-1-4939-7253-1_18).
34. R Core Team. *R: A Language and Environment for Statistical Computing*. R Foundation for Statistical Computing, Vienna, Austria, 2024. URL <https://www.R-project.org/>.
35. Yihui Xie. knitr: A Comprehensive Tool for Reproducible Research in R. In Victoria Stodden, Friedrich Leisch, and Roger D. Peng, editors, *Implementing Reproducible Computational Research*. Chapman and Hall/CRC, 2014.
36. Yihui Xie. *Dynamic Documents with R and knitr*. Chapman and Hall/CRC, Boca Raton, Florida, 2nd edition, 2015. URL <https://yihui.org/knitr/>.
37. Yihui Xie. *knitr: A General-Purpose Package for Dynamic Report Generation in R*. 2024. URL <https://yihui.org/knitr/>.
38. Tyler W. Rinker and Dason Kurkiewicz. *pacman: Package Management for R*. Buffalo, New York, 2018. URL <http://github.com/trinker/pacman>.
39. Tyler Rinker and Dason Kurkiewicz. *pacman: Package Management Tool*. 2019. URL <https://github.com/trinker/pacman>.
40. Thomas Lin Pedersen. *patchwork: The Composer of Plots*. 2024. URL <https://patchwork.data-imaginist.com>.

41. Hadley Wickham. *ggplot2: Elegant Graphics for Data Analysis*. Springer-Verlag New York, 2016. ISBN 978-3-319-24277-4. URL <https://ggplot2.tidyverse.org>.
42. Hadley Wickham, Winston Chang, Lionel Henry, Thomas Lin Pedersen, Kohske Takahashi, Claus Wilke, Kara Woo, Hiroaki Yutani, Dewey Dunnington, and Teun van den Brand. *ggplot2: Create Elegant Data Visualisations Using the Grammar of Graphics*. 2024. URL <https://ggplot2.tidyverse.org>.
43. Kirill Müller and Hadley Wickham. *tibble: Simple Data Frames*. 2023. URL <https://tibble.tidyverse.org/>.
44. Hadley Wickham, Davis Vaughan, and Maximilian Girlich. *tidyr: Tidy Messy Data*. 2024. URL <https://tidyr.tidyverse.org>.
45. Hadley Wickham, Jim Hester, and Jennifer Bryan. *readr: Read Rectangular Text Data*. 2024. URL <https://readr.tidyverse.org>.
46. Hadley Wickham, Romain François, Lionel Henry, Kirill Müller, and Davis Vaughan. *dplyr: A Grammar of Data Manipulation*. 2023. URL <https://dplyr.tidyverse.org>.
47. Hadley Wickham. *stringr: Simple, Consistent Wrappers for Common String Operations*. 2023. URL <https://stringr.tidyverse.org>.